Science and Technology Publishing (SCI & TECH)
ISSN: 2632-1017
Vol. 7 Issue 7, July - 2023

Matlab/Simulink Simulation-Based Modelling And Evaluation Of Three Phase Induction Motor With Varying Load

Akpan, Akaninyene Ndarake[1]
Department of Electrical/Electronic Enig8ineering
Cross River State University of Technology (CRUTECH)
candyguy23@gmail.com

Akpama, Eko James[2]
Department of Electrical/Electronic Enig8ineering
Cross River State University of Technology (CRUTECH)
ekoapkama2004@yahoo.com

***Abstract*— In this paper, MATLAB/Simulink simulation-based modelling and evaluation of three phase induction motor with varying load is presented. Mathematical models of the three phase induction machine based on the system of non-linear ordinary differential and algebraic equations and their DQ transformations are presented. Based on the mathematical models, computer simulations with MATLAB/SIMULINK of the test machines were carried out and the models are used to compare the dynamic behaviours of the three phase induction machines at different operating load conditions. The simulation was conducted using 10.0KW induction motor on no-load with load torque, TL of 0 Nm, on constant load with TL of 50 Nm, on linear load with TL = 0.9 ωr Nm and on two different pump loads. From the result, it was observed that the rated speed on no-load was 1800 rpm, the rotor speed rose to 1700 rpm at the application of a constant load of 50N-m at 0.30s, 1590 rpm at the application of a linear load at 0.5s, 50 rpm at the application of the first pump load and 0 rpm at the application of the second pump load. Also the mechanical rotor speed at no-load rose to 380rad/sec, to 355rad/sec for the constant load, to 330rad/sec for the linear load, to 10rad/sec for the first pump load and to 380rad/sec for the second pump load.**

Keywords: Linear Load, Three Phase Induction Motor, DQ Transformations, Non-Linear Ordinary Differential, Pump Load

1. INTRODUCTION

Over the years, the conventional three phase induction motor drives have found applications in the industries but not without problems related to efficient speed control, fault tolerance, harmonic reduction and overall system integrity [1,2,3]. The induction motor operates at constant load. There is a need for energy-efficiency improvements, process optimization and numerous other environmental benefits and this makes it desirable to operate induction motors for many applications at continuously adjustable speeds as well as various speed torque variations of load [4,5,6]. The result of the application of varying loads on induction motors is that it slows down the speed of the motor, especially the pump load [7,8,9].

Accordingly, this work looks at intermittent loading of the pump loads as one of the ways to improve the performance of the motor [10]. Notably, dynamic modelling of induction motor drive system is essential and commonly used in many industrial settings and it is also used in the evaluation of the motor-drive design process [10,11]. In this way some avoidable design mistakes are avoided. The dynamic model of the induction motor is derived by transferring the three-phase quantities into two-phase direct and quadrature axes quantities. This paper presented the modelling of three phase induction motor with varying load which is simulated using MATLAB/Simulink software. Such modelling and simulations are essential for pre-testing of induction motor drive systems and this approach is used by researchers to determine the appropriate experimental setup that can be adopted for testing the moot drive system. The transient behaviour of an electric machine is of particular importance when the drive system is to be controlled.

Specifically, in this paper, mathematical models of the three phase induction machine based on the system of non-linear ordinary differential and algebraic equations were studied and their DQ transformations were presented. Based on the mathematical models, computer simulations with MATLAB/SIMULINK of the test machines were carried out and the models are used to compare the dynamic behaviours of the three phase induction machines at different operating load conditions.

2. METHODOLOGY

2.1 MODELLING OF INDUCTION MACHINE

A typical dynamic model for induction motors is made up of the electrical sub-model, the torque sub-model and the mechanical sub-model. Furthermore, a stator current output sub-model is needed to determine the voltage drop across the supply cables. A typical induction motor d-q equivalent circuit used for the dynamic modelling equations is shown in Figure 1 for the q-axis model and Figure 2 for the d-axis model. Basically, the induction machine dynamic model is developed using differential equations for the voltages and torque. Notably, the equations for the voltage expressed with respect to various machine variables which are referred to the stator windings are given in Equation 1 [13].

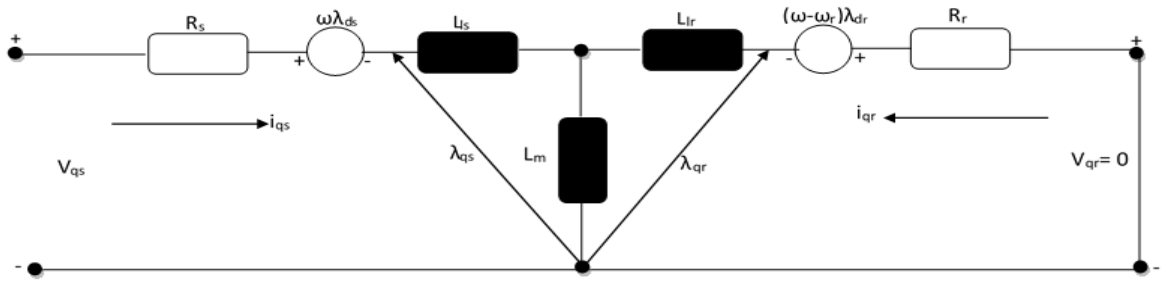

Figure 1: Squirrel-Cage Induction machine models in d-q axis: (a) q-axis model

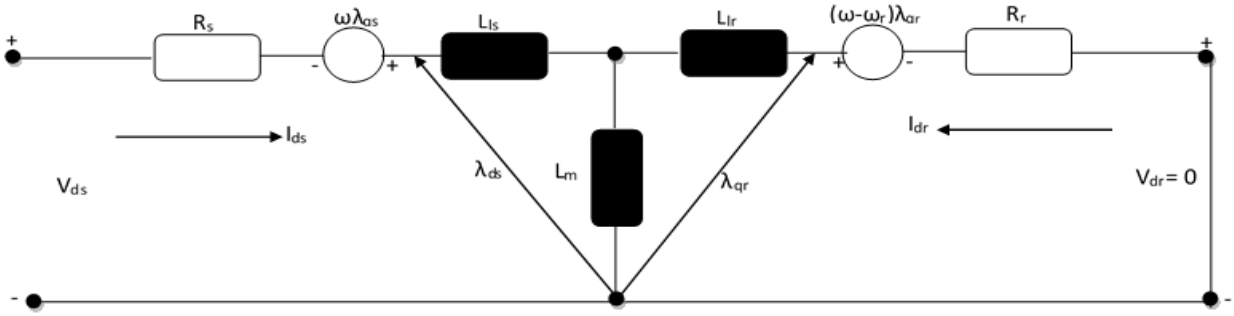

Figure 2: Squirrel-Cage Induction machine models in d-q axis: (b) d-axis model

$$\begin{bmatrix} V_{qs} \\ V_{ds} \\ 0 \\ 0 \end{bmatrix} = \begin{bmatrix} (R_s + L_s p) & -\omega_r L_s & L_m p & \omega_r L_m \\ -\omega_r L_s & (R_s + L_s p) & -\omega_r L_m & L_m p \\ L_m p & 0 & (R_r + L_r p) & 0 \\ 0 & L_m p & 0 & (R_r + L_r p) \end{bmatrix} \begin{bmatrix} i_{qs} \\ i_{ds} \\ i_{qr} \\ i_{dr} \end{bmatrix} \quad (1)$$

The state space representation of equation 1 is given in Equation 2 [14,15];

$$p[i] = -[L]^{-1}([R] + \omega_r[G])[i] + [L]^{-1}[V] \quad (2)$$

where,

d-q voltage matrix [V] is given in Equation 3, stator and rotor current matrix [i] is given in Equation 4, and the other constants matrix [R], [L] and [G] found in Equation 5 are given in Equation 6 and Equation 7 respectively.

$$[V] = \begin{bmatrix} V_{qs} & V_{ds} & 0 & 0 \end{bmatrix}^t \quad (3)$$

$$[i] = \begin{bmatrix} i_{qs} & i_{ds} & i_{qr} & i_{dr} \end{bmatrix}^t \quad (4)$$

$$[R] = \begin{bmatrix} R_s & 0 & 0 & 0 \\ 0 & R_s & 0 & 0 \\ 0 & 0 & R_r & 0 \\ 0 & 0 & 0 & R_r \end{bmatrix} \quad (5)$$

$$[L] = \begin{bmatrix} L_s & 0 & L_m & 0 \\ 0 & L_s & 0 & L_m \\ L_m & 0 & L_r & 0 \\ 0 & L_m & 0 & L_r \end{bmatrix} \quad (6)$$

$$[G] = \begin{bmatrix} 0 & L_s & 0 & L_m \\ -L_s & 0 & -L_m & 0 \\ 0 & 0 & 0 & 0 \\ 0 & 0 & 0 & 0 \end{bmatrix} \quad (7)$$

With respect to the transformed d-q, the electromagnetic torque, Te is expressed as [19] ;

$$T_e = \frac{3}{2} P L_m (i_{qs} i_{dr} - i_{ds} i_{dr}) \quad (8)$$

where, P represents the number of pole pairs,. Then, for a balanced condition, the stator voltages is given as:

$$V_{as} = \sqrt{2} V \cos \omega_b t \quad (9)$$

$$V_{bs} = \sqrt{2} V \cos(\omega_b t - \frac{2\pi}{3}) \quad (10)$$

$$V_{cs} = \sqrt{2} V \cos(\omega_b t + \frac{2\pi}{3}) \quad (11)$$

The stator voltages are related to the d-q frame of reference by equation below

$$\begin{bmatrix} V_{qs} \\ V_{ds} \end{bmatrix} = [C_1] \begin{bmatrix} V_{as} \\ V_{bs} \\ V_{cs} \end{bmatrix} \quad (12)$$

where,

$$C_1 = \frac{2}{3}\begin{bmatrix} \cos\theta, \cos\left(\theta_r - \frac{2\pi}{3}\right) \cos\left(\theta_r - \frac{4\pi}{3}\right) \\ \sin\theta, \sin\left(\theta_r - \frac{2\pi}{3}\right) \sin\left(\theta_r - \frac{4\pi}{3}\right) \end{bmatrix} \quad (13)$$

2.2. MODELLING OF INDUCTION MOTOR WITH VARIATION OF PARAMETERS

The design of induction motor requires the knowledge of the load torque, as well as the start-up and maximum torque generated by the motor. Moreover, variable load induction motor is usually employed in the high performance electrical machine tools, elevators and robots, among others. In this paper, the different load considered in the simulation are:

i. Simulation and analysis of conventional model of 10.0KW induction motor on no-load with T_L = 0 Nm.
ii. Simulation and analysis of conventional model of 10.0KW induction motor on constant load with T_L = 50 Nm.
iii. Simulation and analysis of conventional model of 10.0KW induction motor on linear load with T_L = 0.9 ωr Nm.
iv. Simulation and analysis of conventional model of 10.0KW induction motor on pump load. In the case of the pump load, T_L is given as;

$$T_L = 0\ (t < 1.5\ and\ t \geq 3.0) \quad (14)$$

Notably, the induction motor is connected to two pump loads, namely;

$$T_1 = 8.23\exp(-0.9) + 9.50e(-1) \times \omega_r \text{^}2 \quad (15)$$

$$T_2 = 1.29\exp(0.9) - 4.50e(-1) \times \omega_r \text{^}2 \quad (16)$$

The expressions in Equation14, Equation 15 and Equation 16 are applied in the modelling of the load for the simulation of the performance of the induction motor using computer simulation.

3. RESULTS AND SIMULATION

3.1 SIMULATION RESULTS FOR THE INDUCTION MOTOR ON NO-LOAD

The induction motor was simulated on no-load and the results were obtained as presented in Figure 3 to Figure 7. The graph of rotor speed against time on no-load is shown in Figure 3 and it shows that the rotor speed rises to 1800 rpm at 0.25s immediately after starting and the speed remains steady thereafter. The graph of electromagnetic torque against time on no-load is given in Figure 4 and it shows that the torque runs at zero (0)N-m when started and remains at that level thereafter. The graph of torque against speed on no-load is shown in Figure 5 and it shows that the graph tends to show a cyclic pattern which reduces immediately the speed rises to 1800rpm. The graph of the mechanical rotor speed against time is displayed in Figure 6. The mechanical speed rises to 380rad/s at 0.25s immediately the motor is started and remains steady thereafter. The combined graphs of ias, ibs and ics on no-load is shown in Figure 7. It shows the phase current performances of the motor at no-load.

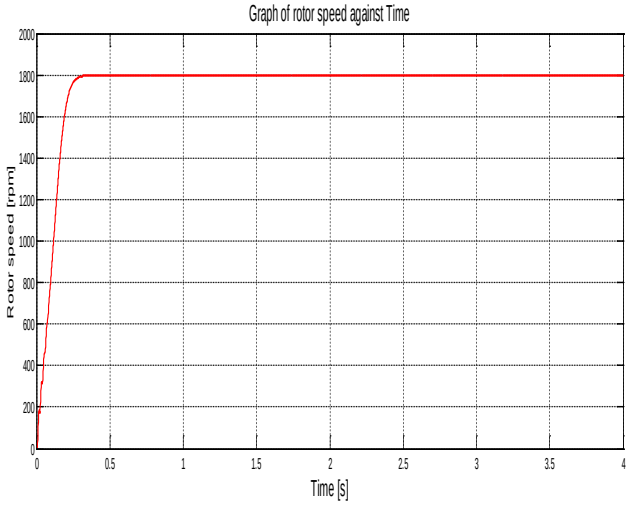

Figure 3 The graph of rotor speed against time on no-load

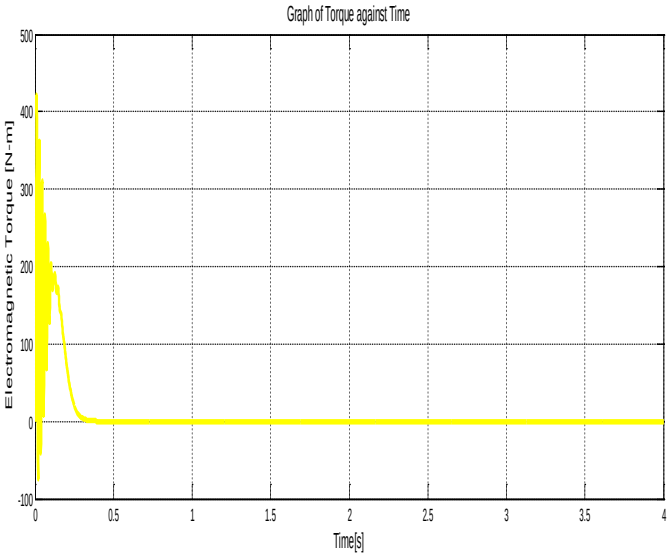

Figure 4: The graph of torque against time on no-load

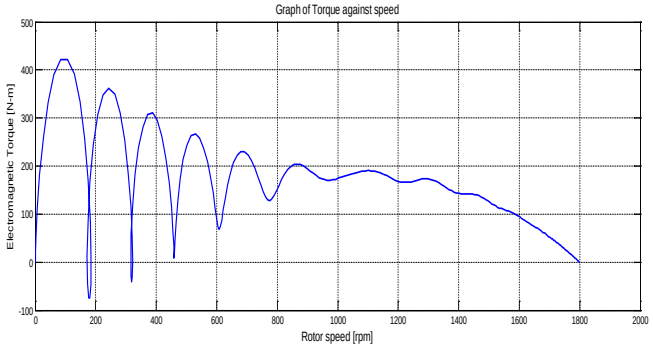

Figure 5: The graph of torque against speed on no load

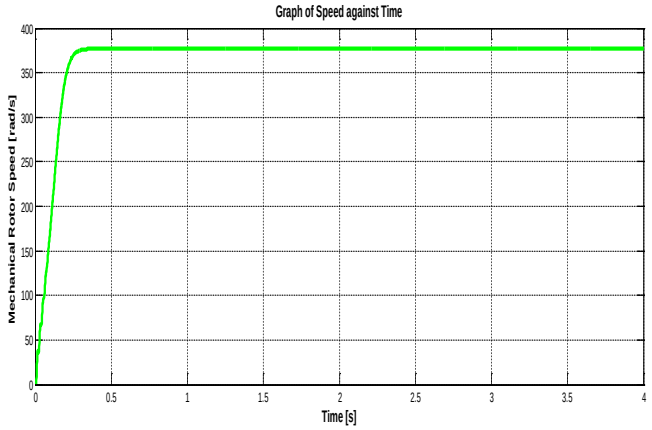

Figure 6: The graph of mechanical rotor speed against time on no-load

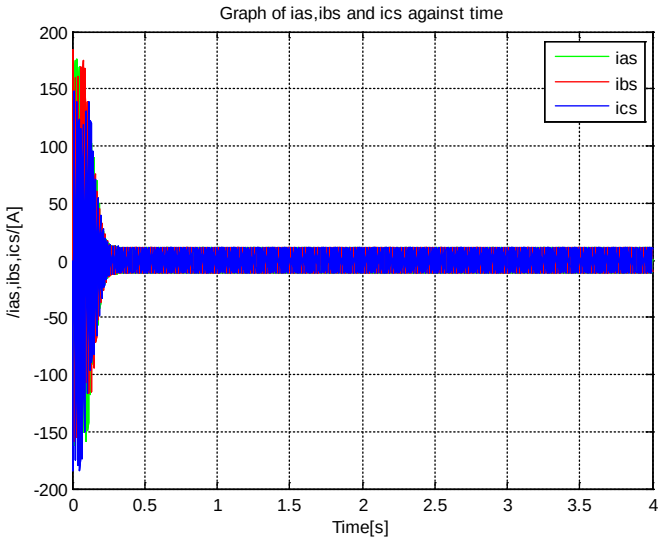

Figure 7: The graph of combined ias, ibs and ics against time on no-load

3.2 SIMULATION RESULTS FOR THE INDUCTION MOTOR ON CONSTANT LOAD

In this section, the induction motor was simulated at constant load and the results were shown in Figure 8 to Figure 12. At constant load, Figure 8 shows that the rotor speed rises to 1700 rpm at the application of a constant load of 50N-m at 0.30s and remains steady thereafter. The torque in Figure 9 becomes 50 N-m at 0.30 immediately after a load of 50 N-m is applied. A cyclic pattern is noticed in Figure 10 when the electromagnetic torque is plotted against the motor speed at the application of a constant load. The graph of mechanical rotor speed against time on constant load is shown in Figure 11 and it shows that the mechanical rotor speed reduces to 355 rad/s immediately after a constant load of 50 N-m is applied to the motor. The mechanical speed remains steady thereafter at that speed. The graph of combined ias, ibs, and ics against time on constant load is shown in Figure 12.

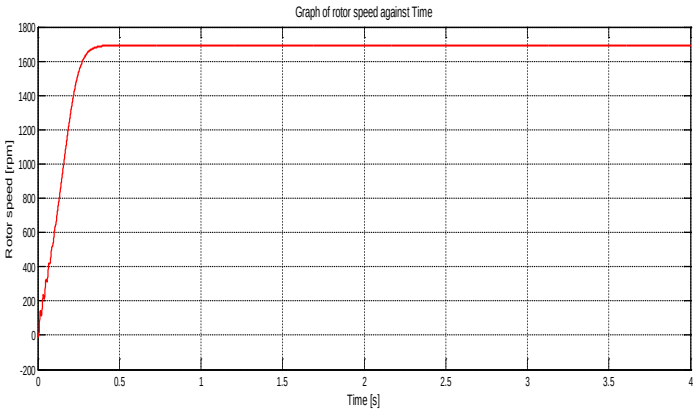

Figure 8: The graph of rotor speed against time on constant load

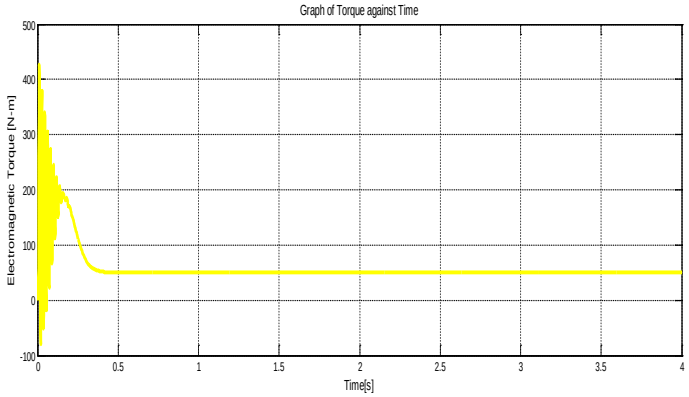

Figure 9: The graph of electromagnetic torque against time on constant load

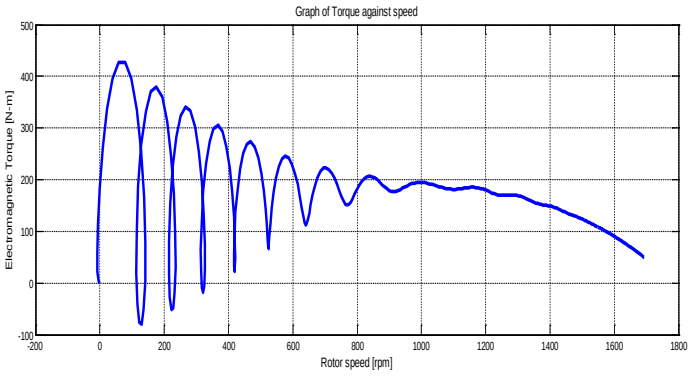

Figure 10: the graph of electromagnetic torque against speed on constant load

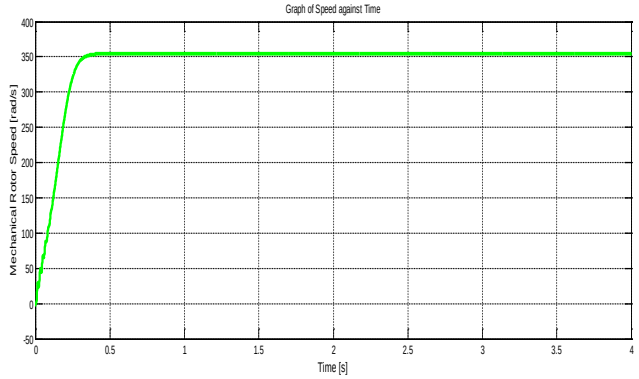

Figure 11: The graph of mechanical rotor speed against time on constant load

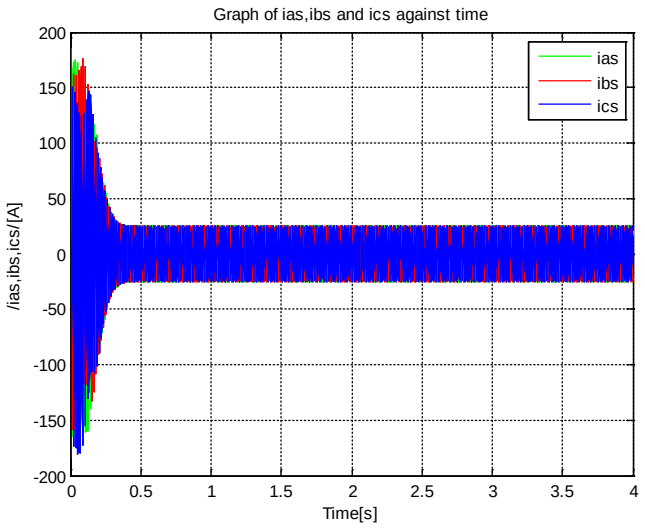

Figure 12: The graph of combined ias, ibs and ics against time on constant load

3.3 SIMULATION RESULTS FOR THE INDUCTION MOTOR ON A LINEAR LOAD

The induction motor was simulated and analysed under linear load and the results were presented in Figure 13 to Figure 17. The rotor speed graph against time is shown in Figure 13 and the graph shows that the rotor speed reduces to 1590 rpm from its rated speed at the application of a linear load at 0.5s. The electromagnetic torque graph against time in Figure 14 shows that the torques becomes 100N-m immediately a linear load is applied on the motor. This torque remains throughout the duration of the operation. The cyclic pattern is also noticed in Figure 15 when electromagnetic torque is plotted against speed at the application of linear load. The pattern fades away when the speed rises to 1590 rpm and becomes steady thereafter. The graph of mechanical rotor speed against time is shown in Figure 16. At the application of a linear load, the mechanical rotor speed reduces to 330rad/s at exactly 0.5s and remains steady thereafter. The combined phase currents i.e ias, ibs, ics is shown in Figure 17.

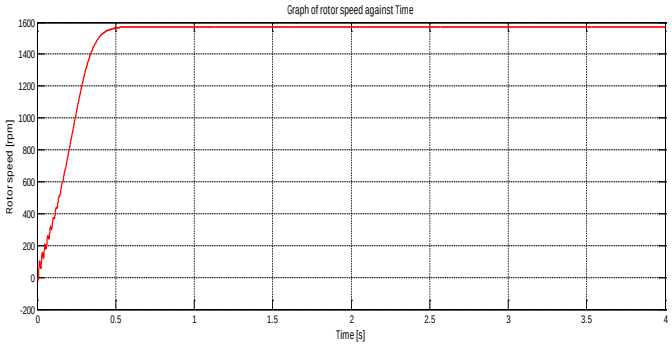

Figure 13: The graph of rotor speed against time on linear load

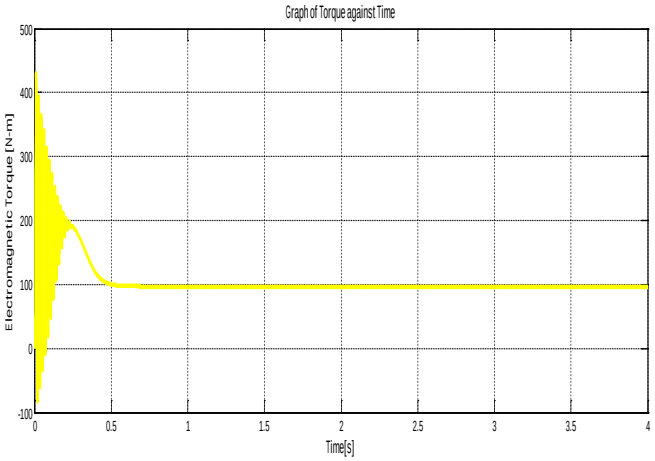

Figure 14: The graph of electromagnetic torque against time on linear load

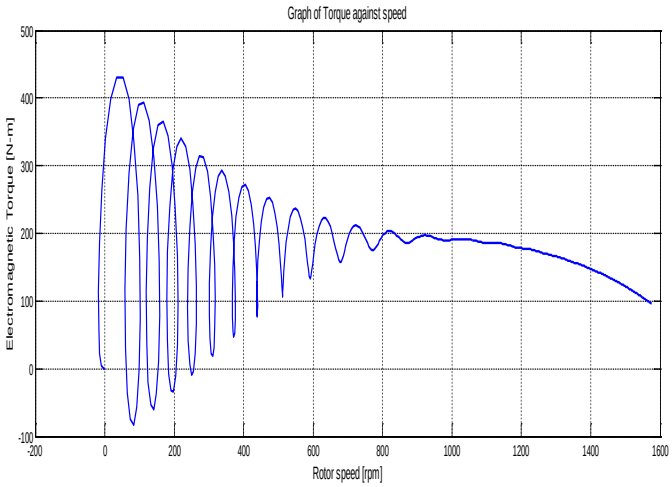

Figure 15: The graph of electromagnetic torque against speed on linear load

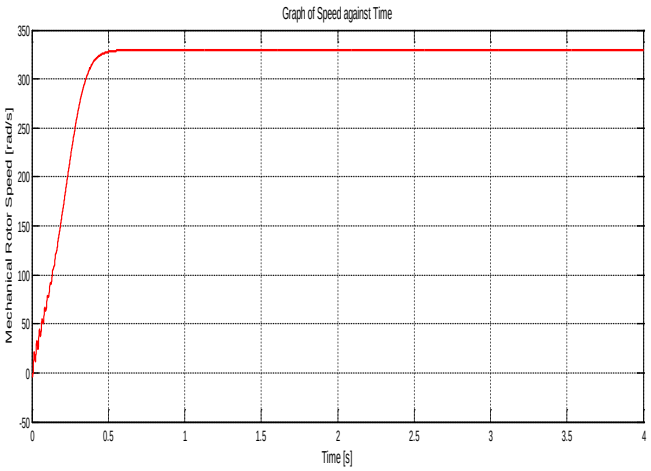

Figure 16: The graph of mechanical rotor speed against time on linear load

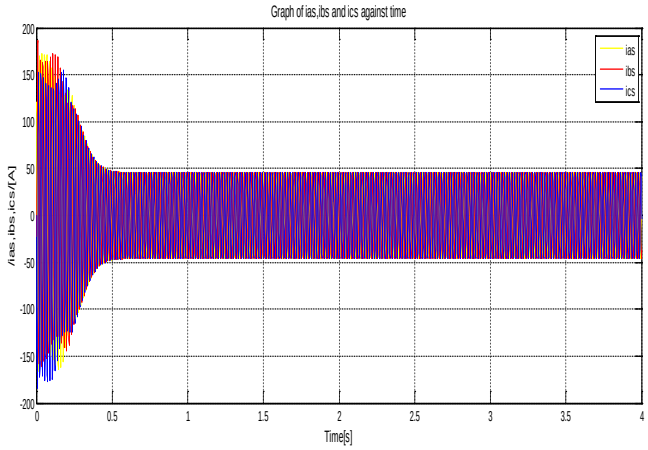

Figure 17: The graph of combined ias, ibs and ics against time on linear load

3.4 SIMULATION RESULTS FOR THE INDUCTION MOTOR ON PUMP LOAD 1 (T1)

The induction motor was simulated and analysed under the first pump load (T1) and the results are presented in Figure 18 to Figure 21. The graph of the rotor speed against time on pump load at the application of pump load $T_1 = 8.23\exp(-0.9) + 9.50e(-1) \times \omega_r \wedge 2$ is shown in Figure 18. This pump load is applied on the motor between 1.5s to 3.0s. The rotor speed reduces to 50 rpm at the application of the pump load and remains steady during the time interval of 1.5s to 3.0s. The graph of electromagnetic torque against time on pump load (T1) is shown in Figure 19, and it shows that the electromagnetic torque reduce to 0Nm at the application of the pump load. The graph of mechanical rotor speed against time on pump load (T1) presented in Figure 20 shows that the mechanical rotor speed reduces to 10 rad/s as seen in the graph of the mechanical speed against time when a load of $T_1 = 8.23\exp(-0.9) + 9.50e(-1) \times \omega_r \wedge 2$ is applied on the motor. This reduction in the rotor speed is between the time of 1.5s to 3.0s. The combined phase current graph of the motor where ias, ibs and ics are plotted on the same graph against time is seen in Figure 21. The transient happens between 1.5s to 3.0s.

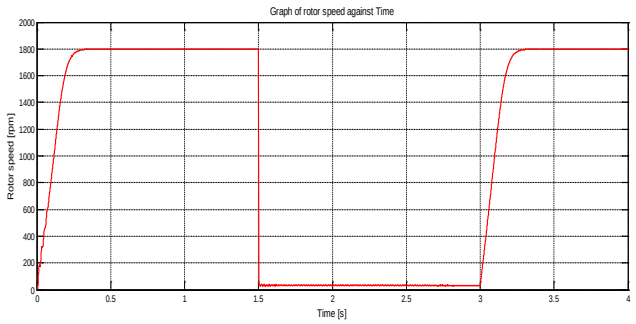

Figure 18: The graph of rotor speed against time on pump load 1 (T1)

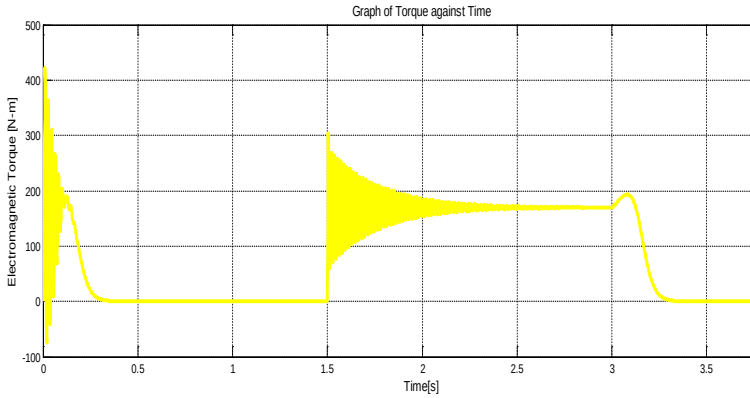

Figure 19: The graph of electromagnetic torque against time on pump load 1 (T1)

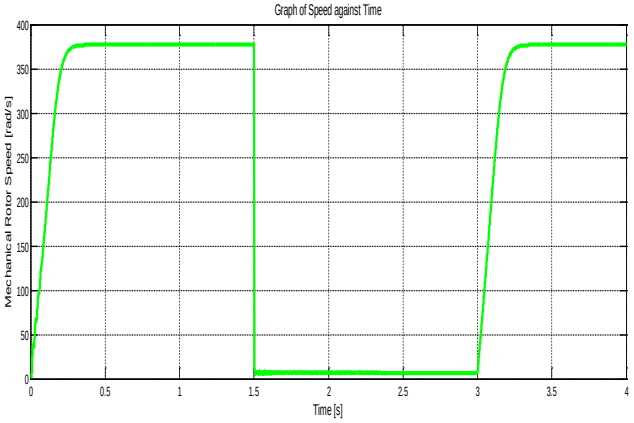

Figure 20: The graph of mechanical rotor speed against time on pump load 1 (T1)

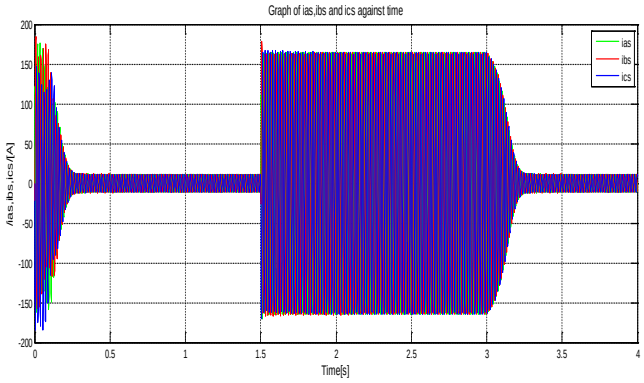

Figure 21: The graph of combined ias, ibs and ics against time on pump load 1(T1)

3.5 SIMULATION RESULTS FOR THE INDUCTION MOTOR ON PUMP LOAD 2 (T2)

The induction motor was simulated and analysed under the second pump load (T2) and the results are presented in Figure 22 to Figure 26. The graph of rotor speed against time at the application of second pump load, T2 given as $T_2 = 1.29\exp(0.9) - 4.50e(-1) \times \omega_r \wedge 2$ is shown in Figure 22. The graph in Figure 20 shows that the motor stops immediately the pump load is applied on the motor. The electromagnetic torque graph against time is shown in Figure 23 and it shows that the electromagnetic torque remains at zero when started. When a load of

$T_2 = 1.29\exp(0.9) - 4.50e(-1) \times \omega_r \wedge 2$ is applied, the motor begins to operate a motor on no-load. The graph in Figure 24 shows the relationship between the mechanical rotor speed and time. The graph exhibit a cyclic nature at the application of $T_2 = 1.29\exp(0.9) - 4.50e(-1) \times \omega_r \wedge 2$ which is the second pump load. The cyclic pattern fades away immediately the speed rises to 1800rpm. The mechanical rotor speed graph against time as seen in Figure 25 shows the speed rising to 380 rad/s but as the pump load of $T_2 = 1.29\exp(0.9) - 4.50e(-1) \times \omega_r \wedge 2$ is applied, the motor speed reduces to zero at 1.5s and the motor stops. The combined graph of ias, ibs and ics against time on pump load 2 (T2) is shown in Figure 26. In the graph, the currents become steady at 0.2s.

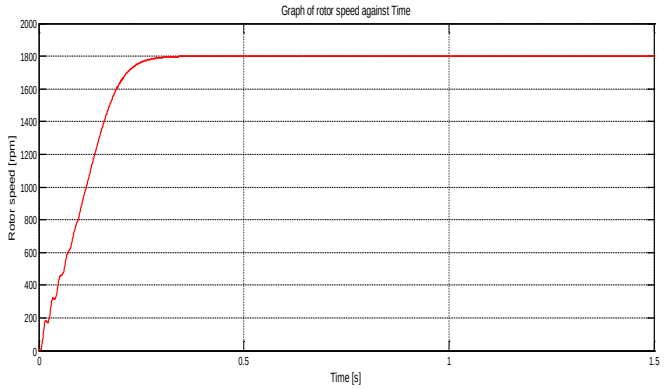

Figure 22: The graph of rotor speed against time on pump load 2 (T2)

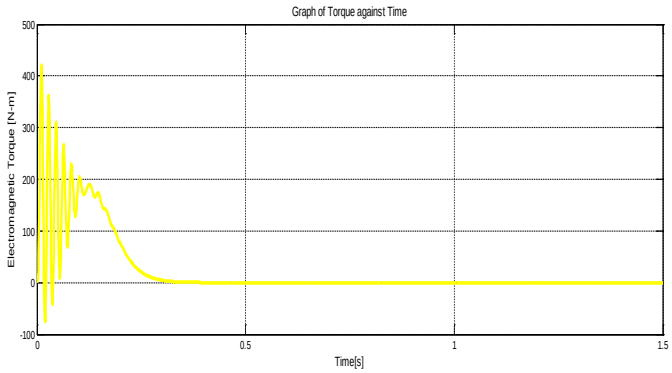

Figure 23: The graph of electromagnetic torque against time on pump load 2 (T2)

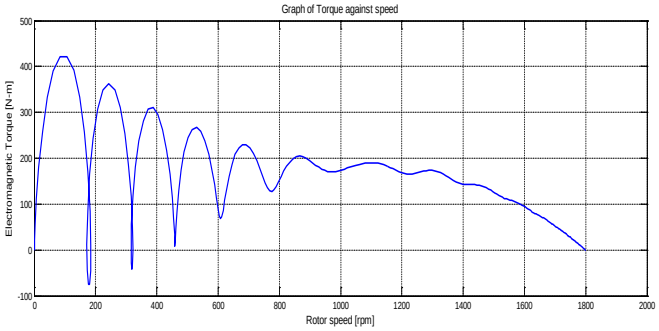

Figure 24: The graph of mechanical rotor speed against time on pump load 2 (T2)

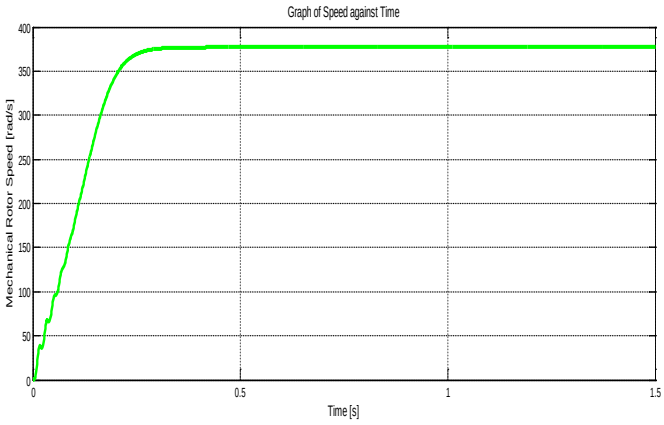

Figure 25: The graph of mechanical rotor speed against time on pump load 2 (T2)

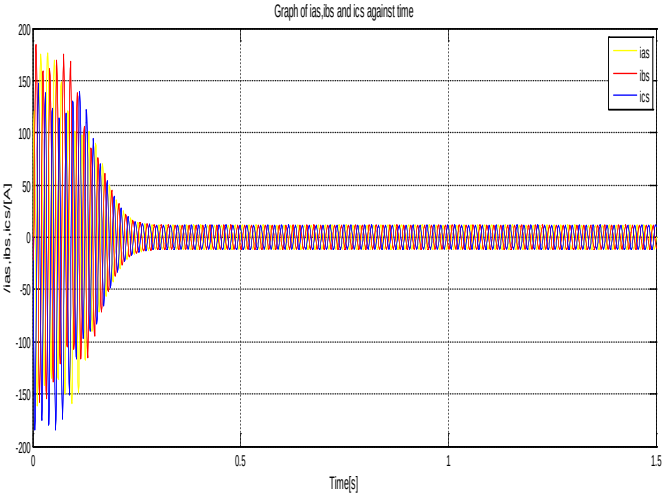

Figure 26: The graph of combined ias, ibs and ics against time on pump load 2 (T2)

4. CONCLUSION

Dynamic models of three phase induction machine based on the system of non-linear ordinary differential and algebraic equations are presented along with their DQ transformations. Based on the mathematical models, computer simulations with MATLAB/SIMULINK of the test machines were carried out and the models are used to compare the dynamic behaviours of the three phase induction machines at different operating load conditions. Specifically, the simulation was conducted using a case study 10.0KW induction motor on no-load, on constant load, on linear load and on two different pump loads. Such modelling and simulations are essential for pre-testing of induction motor drive systems.

REFERENCES

1. Yepes, A. G., Gonzalez-Prieto, I., Lopez, O., Duran, M. J., & Doval-Gandoy, J. (2022). A comprehensive survey on fault tolerance in multiphase ac drives, Part 2: Phase and switch open-circuit faults. *Machines*, *10*(3), 221.
2. Laadjal, K., Bento, F., Henriques, K., Cardoso, A. J. M., & Sahraoui, M. (2023). A Novel Indicator-Based On-Line Diagnostics Technique of Inter-

Turn Short-Circuit Faults in Synchronous Reluctance Machines. *IEEE Journal of Emerging and Selected Topics in Power Electronics*.

3. Sonawane, V. R., & Patil, S. B. (2023). Track and hunt metaheuristic based deep neural network based fault diagnosis model for the voltage source inverter under varying load conditions. *Advances in Engineering Software*, *177*, 103414.
4. Yakhni, M. F., Cauet, S., Sakout, A., Assoum, H., Etien, E., Rambault, L., & El-Gohary, M. (2023). Variable speed induction motors' fault detection based on transient motor current signatures analysis: A review. *Mechanical Systems and Signal Processing*, *184*, 109737.
5. Mohammed, A. N., & Ghoneim, G. A. R. (2021, February). Fuzzy-PID speed controller model-based indirect field oriented control for induction motor. In *2020 International Conference on Computer, Control, Electrical, and Electronics Engineering (ICCCEEE)* (pp. 1-6). IEEE.
6. Mahfoud, S., DEROUICH, A., el Ouanjli, N. A. J. I. B., & EL MAHFOUD, M. O. H. A. M. M. E. D. (2022). Enhancement of the direct torque control by using artificial neuron network for a doubly fed induction motor. *Intelligent Systems with Applications*, *13*, 200060.
7. Hasanah, R. N., Nurwati, T., Ardhenta, L., Suyono, H., & Muljadi, E. (2023, April). Energy Saving during Induction Motor Starting under Loaded Conditions. In *2023 IEEE Green Technologies Conference (GreenTech)* (pp. 112-117). IEEE.
8. Mobarra, M., Tremblay, B., Rezkallah, M., & Ilinca, A. (2020). Advanced control of a compensator motor driving a variable speed diesel generator with rotating stator. *Energies*, *13*(9), 2224.
9. Wati, T., Masfufiah, I., Suheta, T., Putra, N. P. U., & Munir, M. (2021, October). Dynamic Braking of Three Phase Induction Motor Using Inject DC Voltage and Capacitor Load. In *2021 Fourth International Conference on Vocational Education and Electrical Engineering (ICVEE)* (pp. 1-4). IEEE.
10. Feng, Z. M., Guo, C., Zhang, D., Cui, W., Tan, C., Xu, X., & Zhang, Y. (2020). Variable speed drive optimization model and analysis of comprehensive performance of beam pumping unit. *Journal of Petroleum Science and Engineering*, *191*, 107155.
11. Miao, Z., & Fan, L. (2008). The art of modeling and simulation of induction generator in wind generation applications using high-order model. *Simulation Modelling Practice and Theory*, *16*(9), 1239-1253.
12. Bellure, A., & Aspalli, M. S. (2015). Dynamic dq model of induction motor using simulink. *International Journal of Engineering Trends and Technology (IJETT)*, *24*(5), 252-257.
13. Deb, P. B., & Sarkar, S. (2016). Dynamic model analysis of three phase induction motor using Matlab/Simulink. *International Journal of Scientific & Engineering Research*, *7*(3), 572-577.
14. Yaabari, N., Okoro, O. I., & Akpama, E. J. (2022). Matlab-based simulations of a three-phase induction motor for dynamic studies. *Nigerian Journal of Technology*, *41*(6), 1000-1007.
15. Wade, S. Dunnigan,M. W.,Williams,B. W. "Modelling and simulation of induction machine vector control with rotor resistance identification",IEEE Transactions on Power Electronics, vol. 12, No. 3,1997.